Preliminary Petrology and Chemistry of Proximal Eruptive Products: 1992 Eruptions of Crater Peak, Mount Spurr Volcano, Alaska

By Michelle L. Harbin, Samuel E. Swanson, Christopher J. Nye, and Thomas P. Miller

CONTENTS

ABSTRACT

The 1992 eruptions of Crater Peak, Mount Spurr, Alaska, produced two types of andesite distinguished macroscopically by color and texture. The two andesites also have slight petrographic differences. The mineral assemblage of plagioclase, orthopyroxene, clinopyroxene, amphibole, and FeTi oxides is the same for both andesites, and compositions of the mineral phases are nearly identical. However, the color and composition of the groundmass glass differ; one type is brown and andesitic (60–62 weight percent SiO_2) and the other type is colorless and rhyolitic (73–75 weight percent SiO_2). Intermediate dacitic glass compositions are also present. The stability of hornblende phenocrysts also differs between the andesites. In the andesite containing brown andesitic glass, hornblende typically shows little or no reaction corona, whereas in andesite with rhyolitic groundmass glass hornblende phenocrysts have well-developed coronas. Xenoliths of partially melted metamorphic rocks were also ejected during the eruptions.

INTRODUCTION

Mount Spurr, Alaska, located approximately 125 km west of Anchorage, is the northernmost historically active volcanic center of the eastern Aleutian arc. Prehistoric Mount Spurr was an andesitic stratovolcano that underwent avalanche caldera formation approximately 10,000 years ago (Nye and Turner, 1990). Following subsequent ash flows, a dacite dome was emplaced in the caldera and now forms the summit of Mount Spurr. Crater Peak, a flank vent, was built in the breach of the southern caldera rim and has been the site of historic volcanism, including the eruptions in 1953 and 1992.

The 1992 eruptions were subplinian (after Fisher and Schmincke, 1984) and occurred on June 27, August 18, and September 16–17. Each eruption lasted 3.5 to 4 hours (AVO, 1993; Eichelberger and others, this volume). Most of the eruptive material consisted of tephra fall (Neal and others, this volume; Swanson and others, this volume); pyroclastic flows (Miller and others, this volume), debris flows (Meyer and others, this volume), and ballistic showers (Waitt and others, this volume) were less significant. This study concentrates on juvenile blocks emplaced either as bombs or as clasts in the pyroclastic flows during all three eruptions (table 1). Originally, there was some debate as to whether juvenile material was ejected during the June eruption. However, presence of fresh vesicular glass fragments in the distal tephra fall (Swanson and others, this volume), small pumice lapilli, and geochemistry (Nye and others, this volume) indicate that juvenile magma was indeed erupted. Recycling of 1953 olivine-bearing material may be reflected in two olivine-bearing samples—one collected from the June deposits, and one collected from a September pyroclastic flow. The ejecta have been broadly classified into three groups, two of which are juvenile andesite on the basis of hand-sample characteristics. The first group consists of brown-black, breadcrusted, cauliflower-shaped andesite (approximately 95 percent by

Table 1. Eruption date, location and description, and bulk and groundmass glass weight percent SiO_2 of individual andesite samples from 1992 eruptions of Mount Spurr, Alaska.

[Bulk-rock data from Nye and others, this volume. Average values for both bulk-rock and groundmass glass normalized to 100 percent. NA, not analyzed]

Samwle number	Eruption date	Location and description	SiO_2 content bulk rock	SiO_2 content groundmass glass
92JBS-01	June 27	Dense, brown, cauliflower-shaped andesite bomb (23 cm in diameter)	56.68	61.74±0.84
92JBS-03A	June 27	Black rounded breadcrusted andesite bomb (8 cm in diameter)	56.61	61.36±0.85
92JBS-04A	June 27	White pumice lapilli (1 cm in diameter)	NA	74.85±0.54
92JBS-04B1	June 27	Pumice lapilli (1 cm in diameter)	NA	77.04±1.49
92JBS-04B2	June 27	Pumice lapilli (1 cm in diameter)	NA	68.05±2.27; 72.31±1.63
92JBS-04B3	June 27	Pumice lapilli (1 cm in diameter)	NA	61.02±0.77; 77.18±1.65
92CNS-03B	June 27	Rounded breadcrusted (cauliflower-shaped) andesite bomb (8 cm in diameter) from north side of Crater Peak (2,149 m elevation)	NA	60.59±0.98
92MHS-12	Aug. 18	Brown cauliflower-shaped andesite (9 cm in diameter) from pyroclastic flow (762 m elevation)	NA	62.18±0.78
92AMm-101	Aug. 18	Brown andesite from pyroclastic flow	56.45	60.44±0.64
92AMm-102GS	Aug. 18	Greenish colored scoria from fallout	56.59	65.87±1.60
92AMm-111A-1	Aug. 18	Pumiceous metamorphic clast	60.15	73.42±0.67
92AMm-111A-3	Aug. 18	Pumiceous metamorphic clast	66.68	74.44±0.75
92AMm-111B	Aug. 18	Brown andesite from east side of Crater Peak	56.50	61.82±1.00
92AMm-113A	Aug. 18	Pumiceous metamorphic material from pyroclastic flow on the south side of Crater Peak	65.02	74.97±0.90
92AMm-113C	Aug. 18	Sugary, grayish-green andesite from pyroclastic flow on the south side of Crater Peak	58.84	75.56±0.38
92AMm-120A	Sept. 17	Grayish-green prismatic andesite from 1,402 m elevation on the west tongue of Kidazgeni Glacier	56.52	74.03±1.24
92AMm-120B	Sept. 17	Dark-gray to black prismatic andesite from 1,402 m elevation on the west tongue of Kidazgeni Glacier	56.54	67.47±1.68
92AMm-129a	Sept. 17	Dark-gray to black andesite from 1,829 m elevation of Kidazgeni Glacier	57.19	64.36±1.18
Stop 35	Sept. 17	Brown vesicular andesite from 1,402 m elevation of Kidazgeni Glacier	57.85	62.34±1.04; 64.60±0.83 65.44±0.70
920924-3	Sept. 17	Dense, dark-gray to black andesite from 1,402 m elevation of Kidazneni Glacier	56.62	64.72±1.06
920926-6	Sept. 17	Dark-gray to black andesite from 1.402 m elevation of Kidazgeni Glacier	57.05	64.35±1.37

volume of pyroclastic flows). The second group consists of greenish-gray andesite (approximately 1 percent by volume of pyroclastic flows) erupted in August and September. The third group consists of xenoliths and old volcanic rocks (approximately 4–5 percent by volume of pyroclastic flows) (Miller and others, this volume).

PETROLOGY AND CHEMISTRY

Petrographically, the andesite of the first two groups are nearly identical. Both contain phenocrysts of plagioclase, orthopyroxene, clinopyroxene, hornblende, and FeTi oxides. One difference between the andesites is the groundmass glass. The brown andesite has a groundmass of very microlite-rich (plagioclase, pyroxene, FeTi oxides) brown glass. The greenish-gray andesite has a colorless groundmass glass with or without microlites. The other striking difference between the two andesite types is the apparent stability of hornblende phenocrysts. Hornblende in the brown andesite does not have reaction coronas, but hornblende phenocrysts in the greenish-gray andesite have well-developed reaction coronas.

Metamorphic xenoliths are present in small pumice lapilli from the June eruption and as large blocks in the pyroclastic flows and bomb fields of August and September. These xenolithic blocks are as much as 50 cm in maximum diameter and typically are highly inflated (40–60 percent vesicles). Phases represented in the xenoliths include vesicular colorless rhyolitic glass, quartz, plagioclase, pyrrhotite±orthopyroxene ±cordierite±spinel±magnetite±ilmenite±sillimanite ±biotite±garnet±apatite±graphite±corundum.

ANALYTICAL TECHNIQUES

Analyses of polished thin sections were performed on the four-channel electron microprobe at the University of Alaska, Fairbanks. Mineral analyses were done using an accelerating voltage of 15 Kev, a beam current of 10 nA, a beam diameter of 5 μm, and a counting time of 10 sec per element. Well-characterized natural minerals were used as standards. Glass analyses were done at 15 Kev, 10 nA, 8 μm, and a 10-sec counting time per element. Natural glasses were used as standards for all major elements. The scapolite standard was used as a standard for chlorine. This analytical routine was designed to minimize Na loss during analysis of these glasses. Analysis of Redoubt Volcano samples using this same analytical routine (Swanson and others, 1994) indicates no significant loss of Na during an analysis when Na is measured within the first 10 seconds of the analysis. Analyses that clearly included mineral grains were eliminated from the data set. Statistical tests were then performed on the data set to develop a good total range of acceptable analyses. The microlite-rich glasses were the most contaminated, and some of the heterogeneity of these glasses can be attributed to the presence of the microlites.

GROUNDMASS GLASS

The brown-black andesite of the June and August eruptions contains a microlite-rich brown glass, but most samples from the September eruption and some from the August eruption contain a microlite-rich, lighter-brown glass. However, it is nearly impossible to macroscopically identify samples with the light-brown glass because they are similar to samples with a brown groundmass glass in August deposits, but the clasts from September are lighter in color. August and September ejecta also contain greenish-gray andesite with a colorless groundmass glass.

Color differences among the groundmass glass types identified to date correlate with differences in the composition of the glass. Compositionally, the brown microlite-rich glass from the June and August eruptions is andesitic (60–62 weight percent SiO_2) (fig. 1, table 2). Small pumice lapilli on the surface of the June deposits contain brown andesitic (60–62 weight percent SiO_2) (the same as that in the large brown-black blocks) and dacitic (65–71 weight percent SiO_2) glass and colorless glass that is dacitic (68–73 weight percent SiO_2) and rhyolitic (75–79 weight percent SiO_2) in composition. The boundaries between the two glasses are sharp. One sample from the August eruption has a light-brown microlite-rich glass that is dacitic (approximately 65 weight percent SiO_2).

Brown-black andesite from the September eruption is lighter in color and contains lighter, more silicic groundmass glass relative to that of the June and August brown-black andesite. September glasses are mostly dacitic (63–68 weight percent SiO_2) (fig. 1, table 2) but show a wide compositional range among and within samples. This change in dominant glass composition was also observed in analyses of distal tephra fall (Swanson and others, this volume).

One sample from September (Stop 35, table 1) contains all three colors of glass (brown, light brown, and colorless) with diffuse contacts between the three glasses; some of the brown glass has an andesitic composition similar to that of June and August samples (table 2), and some is more similar to the light-brown glass in the sample. Both the light-brown glass and colorless glass are dacitic, but the light-brown glass

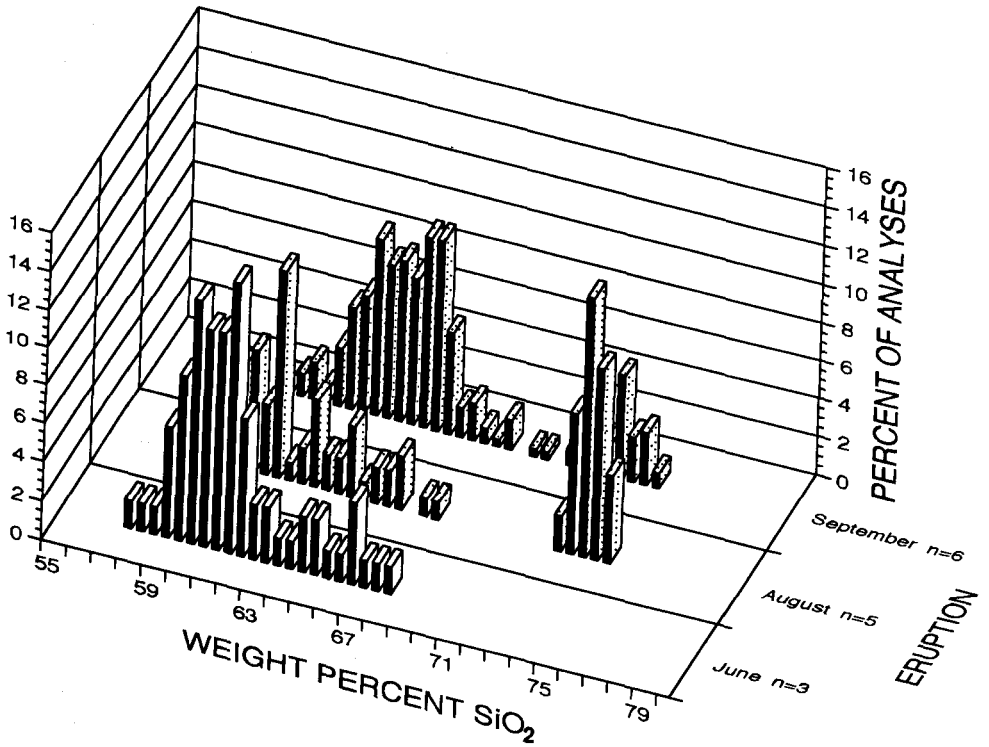

Figure 1. Histogram of groundmass glass compositions analyzed for each of three eruptions of Mount Spurr volcano, Alaska. June and August brown glasses are nearly identical, but the peak is shifted toward more silicic compositions in September. The August and September colorless glasses are also nearly identical. "Percent of Analyses" is the percentage of total analyses of a given weight percent SiO_2. The total number of analyses varies for each eruption, 71 for June samples, 111 for August, and 261 for September. n, number of samples analyzed from each eruption.

Table 2. Average groundmass glass compositions for andesite from 1992 eruptions of Mount Spurr volcano, Alaska.

[*, total Fe as Fe_2O_3; n, number of analyses; †, sample from June eruption; ‡, sample from August eruption; §, sample from September eruption]

	Andesite glass				Dacite glass			Rhyolite glass	
	92JBS01†	92JBS03A†	92AMm111B‡	Stop 35§	92AMm102GS‡	92AMm129a§	92AMm120B§	92AMm113C‡	92AMm120A§
SiO_2	60.39±1.63	61.34±0.81	60.98±0.89	61.65±0.80	65.24±2.04	63.27±1.36	67.08±1.61	74.28±0.54	73.46±1.27
TiO_2	0.67±0.12	0.66±0.18	0.65±0.18	0.50±0.07	0.48±0.15	0.56±0.21	0.60±0.18	0.39±0.16	0.26±0.12
Al_2O_3	16.24±0.60	15.95±0.71	15.44±1.11	16.2 ±0.41	15.76±1.53	15.86±0.93	14.61±1.07	12.21±0.14	13.41±1.01
Fe_2O_3*	6.92±0.69	7.64±0.63	7.34±0.90	7.03±1.20	5.24±1.03	6.09±0.90	5.34±0.82	2.68±0.21	2.49±0.40
MgO	2.14±0.43	2.33±0.67	2.80±0.94	2.26±0.32	1.21±0.70	1.75±0.46	0.94±0.45	0.39±0.03	0.26±0.04
CaO	5.61±0.31	5.73±0.33	5.34±0.48	5.09±0.35	4.35±0.92	4.50±0.55	3.67±0.64	1.36±0.19	1.57±0.67
Na_2O	4.38±0.17	4.91±0.25	4.54±0.29	4.45±0.19	4.75±0.37	4.50±0.26	4.85±0.29	3.72±0.15	4.41±0.26
K_2O	0.67±0.12	0.66±0.18	0.65±0.18	0.50±0.07	1.80±0.23	1.59±0.20	2.14±0.31	2.96±0.08	3.02±0.28
Cl	0.12±0.04	0.21±0.04	0.16±0.04	0.17±0.04	0.21±0.04	0.18±0.04	0.20±0.05	0.33±0.04	0.35±0.07
Total	97.81f1.83	99.97M.53	98.65±0.69	98.9W1.36	99.04M.95	98.31f1.30	99.42±0.51	98.31f0.56	99.23k0.62
n	14	44	24	7	22	38	32	46	44

is slightly less Si rich. The three glasses also contain different microlite abundances. The brown glass is very rich in microlites, the light brown glass has abundant microlites, and the colorless glass is relatively free of microlites.

Blocks of greenish-gray andesite in August and September ejecta have a colorless groundmass glass that is rhyolitic (73–75 weight percent SiO_2) and peraluminous (table 2). The sample from the August eruption contains no microlites in the groundmass glass, but the sample from the September eruption has abundant microlites.

MINERALOGY

PLAGIOCLASE

The modal percentage of plagioclase ranges from approximately 17 to 31 percent (dense rock). It makes up 70 to 90 percent of the phenocrysts, and it typically occurs as euhedral crystals as much as 1 mm long with normal, reverse, oscillatory, and patchy zoning. Sieved (abundant glass inclusions) cores or zones parallel to grain boundaries are very common in phenocrysts.

Rim compositions vary over the eruption sequence and correlate with the composition of the groundmass glass; rhyolitic glass samples contain the more sodic compositions. In June samples, rims range from An_{82} to An_{56}, in August samples, they range from An_{84} to An_{22}, and in September samples, they range from An_{64} to An_{27} (fig. 2A, table 3). Samples from throughout the eruption series that contain similar groundmass glasses have similar compositional ranges. A range of An_{84} to An_{55} characterizes andesitic glass, An_{65} to An_{50} characterizes dacitic glass, and An_{75} to An_{22} characterizes rhyolitic glass (fig. 2B).

CLINOPYROXENE

Light-green, weakly pleochroic clinopyroxene phenocrysts make up less than 1 percent of the mode (dense rock) in both andesite types. Crystals are subhedral to euhedral and less than 0.5 mm in length. The restricted compositional range of $En_{38–48}$ $Fs_{14–19}$ $Wo_{36–44}$ (rim compositions) (fig. 3, table 3) is nearly identical to that of prehistoric Mount Spurr clinopyroxene (Nye and Turner, 1990). There is no clear change in composition with changing groundmass glass composition nor any compositional change through the eruption series.

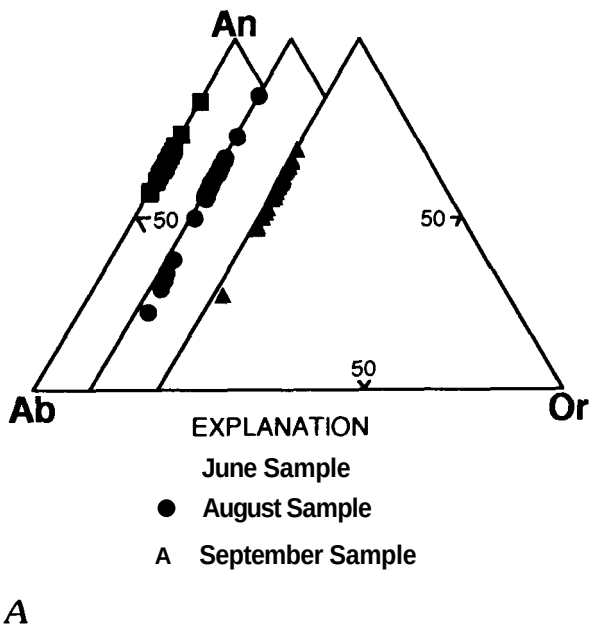

A

Figure 2. A, Range of plagioclase rim compositions of andesites for each of the 1992 Mount Spurr eruptions.

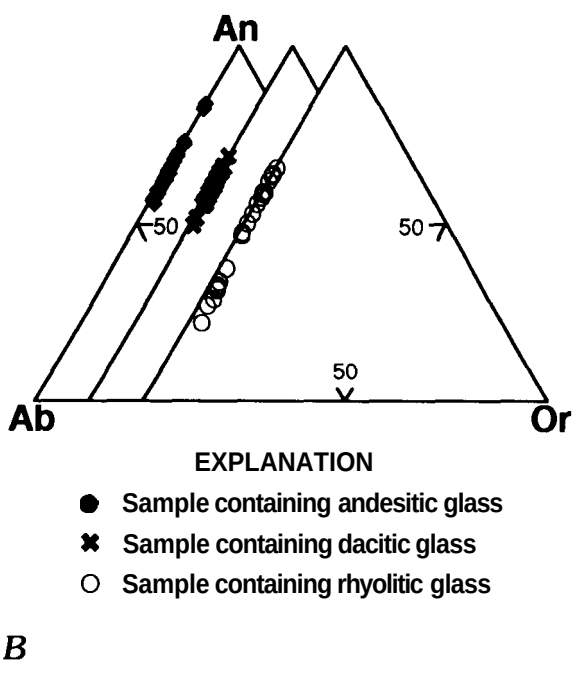

B

Figure 2. Continued. B, Range of plagioclase rim compositions for different groundmass glass compositions.

Table 3. Representative analyses of plagioclase and clinopyroxene of andesites from 1992 eruptions of Mount Spurr volcano, Alaska.

[*. total Fe as Fe_2O_3; pyroxene recalculation scheme from Lindsley (1983) and represents rim compositions; FeO_t, total measured iron as FeO; Mg#, Mg/(Mg+Fe)•100; †, sample from June eruption; ‡, sample from August eruption; §, sample from September eruption]

Plagioclase

	92JBS01†	92AMm111B‡	92AMm102GS‡	92AMm113C‡	92AMm129a§	92AMm120A§
SiO_2	49.39	50.34	46.89	58.90	46.84	53.88
Al_2O_3	32.27	31.29	33.98	26.04	33.69	28.52
Fe_2O_3*	0.52	0.66	0.50	0.19	0.29	0.56
CaO	14.92	13.44	16.45	7.19	16.54	10.97
Na_2O	2.86	3.44	2.15	6.93	2.15	5.20
K_2O	0.03	0.01	0.02	0.34	0.04	0.08
Total	99.99	99.18	99.99	99.60	99.57	99.21
An	74.11	68.25	80.76	35.68	80.75	53.61
Ab	25.69	31.64	19.14	62.25	19.05	45.99
Or	0.20	0.10	0.10	2.07	0.20	0.40

Clinopyroxene

	92JBS03A†	92CNS03B†	92AMm111B‡	92AMm102GS‡	92AMm113C‡	92AMm120A§
SiO_2	50.33	51.89	52.41	52.17	51.73	52.11
TiO_2	0.54	0.38	0.37	0.44	0.44	0.35
Al_2O_3	3.28	2.00	1.95	2.40	2.42	1.70
Fe_2O_3	2.79	1.63	1.04	0.55	1.37	1.51
FeO	6.74	7.40	8.70	8.47	7.56	8.23
MnO	0.41	0.43	0.28	0.32	0.30	0.42
MgO	15.72	16.30	16.97	15.72	15.36	16.32
CaO	20.03	19.78	18.24	19.79	20.66	19.27
Na_2O	0.33	0.26	0.27	0.26	0.35	0.26
Total	100.17	100.07	100.23	100.12	100.19	100.17
FeO_t	9.25	8.87	9.64	8.96	8.79	9.59
En	44.23	45.61	47.59	44.71	43.48	45.58
Fs	15.25	14.60	15.62	14.82	14.45	15.70
Wo	40.52	39.79	36.79	40.47	42.07	38.71
Mg#	74.36	75.75	75.29	75.11	75.06	74.38

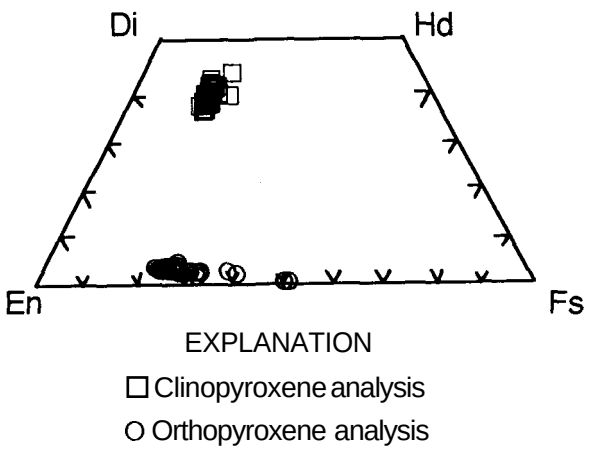

Figure 3. Representative range of clinopyroxene and orthopyroxene rim compositions of andesite samples from three eruptions of Mount Spurr, Alaska, in 1992. Di, diopside; Hd, hedenbergite; En, enstatite; Fs, forsterite.

ORTHOPYROXENE

Orthopyroxene phenocrysts are the most abundant mafic phase in all andesite samples, typically 3 to 7 percent of the mode (dense rock). Crystals are subhedral to euhedral and as much as 1.2 mm long, pale greenish-brown, and weakly to moderately pleochroic. Some crystals have zones (typically cores) that are more strongly colored. The abundance of such "cored" crystals appears to increase in samples from each succeeding eruption. The wide compositional range of En_{49-74} Fs_{22-51} $Wo_{0.3-5}$ (rim compositions) (fig. 3, table 4) is similar to that for prehistoric orthopyroxene (Nye and Turner, 1990). Unlike clinopyroxene, the orthopyroxene shows a compositional change with groundmass glass composition. Orthopyroxene phenocrysts in andesitic and dacitic glass samples have a similar range of En_{61-74} Fs_{22-37} $Wo_{0.9-5}$, but rhyolitic

glass samples contain orthopyroxene with more iron -rich compositions (En_{49-73} Fs_{24-51} $Wo_{0.3-5}$).

AMPHIBOLE

Pargasitic amphibole phenocrysts (Hawthorne, 1981) form less than 2 percent of the mode (dense rock) in all samples. Crystals are euhedral to anhedral, less than 2 mm in largest dimension, and pleochroic in shades of green and brown. Coronas of plagioclase, orthopyroxene, and FeTi oxides surround amphibole in some samples and presumably record disequilibrium. Well-developed coronas are dominant in samples with a colorless rhyolitic groundmass glass, whereas samples containing brown groundmass glass typically lack evidence of disequilibrium. However, amphibole both with and without coronas are found in some samples. Compositionally, the amphibole is high in Al (Al(IV) = 1.35–2, based on 23 oxygens) and alkalies (Na + K in A site = 0.6–0.85) (table 4), similar to the range for prehistoric Mount Spurr amphibole (Nye and Turner, 1990). Pargasitic Mount Spurr amphibole falls at the end of the Aleutian amphibole trend (Kay and Kay, 1985) and is similar to other eastern Aleutian pargasitic amphibole (from Augustine Volcano (Daley, 1986) and Redoubt Volcano (Swanson and others, 1994)) (fig. 4).

Table 4. Representative analyses of orthopyroxene and hornblende of andesite from 1992 eruptions of Mount Spurr volcano, Alaska.

[Pyroxene recalculation scheme from Lindsley (1983) and represents rim compositions; FeO_t, total measured iron as FeO; Mg#, Mg/(Mg+Fe)•100; †, sample from June eruption; ‡, sample from August eruption; §, sample from September eruption]

Orthopyroxene

	92JBS03A†	92CNS03B†	92AMm111B‡	92AMm102GS‡	92AMm113C‡	92AMm120A§
SiO_2	53.21	54.21	53.17	53.04	51.31	52.01
TiO_2	0.19	0.12	0.16	0.26	0.19	0.16
Al_2O_3	1.66	0.96	1.09	1.90	1.25	2.53
Fe_2O_3	1.87	1.33	1.47	1.32	0.18	2.00
FeO	13.82	13.86	16.62	14.79	25.39	15.69
MnO	0.63	0.47	0.69	0.52	0.77	0.51
MgO	26.58	27.54	25.54	26.29	19.24	25.32
CaO	2.11	1.49	1.20	1.62	0.87	1.49
Na_2O	0.03	0.06	0.00	0.00	0.01	0.00
Total	100.10	100.04	99.94	99.74	99.21	99.71
FeO_t	15.50	15.06	17.94	15.98	25.55	17.49
En	71.54	73.78	69.29	71.61	55.54	69.37
Fs	24.38	23.35	28.37	25.23	42.65	27.69
Wo	4.08	2.87	2.34	3.16	1.81	2.94
Mg#	74.58	75.96	70.95	73.95	56.57	71.47

Hornblende

	92CNS03B†	92AMm111B‡	92AMm102GS‡	92AMm113C‡	92AMm120B§
SiO_2	42.84	42.94	42.87	42.64	43.36
TiO_2	2.14	2.39	2.70	2.61	2.38
Al_2O_3	13.51	12.74	11.23	11.92	12.45
FeO_t	10.64	12.69	12.60	12.85	12.09
MnO	0.07	0.11	0.27	0.15	0.30
MgO	15.01	13.34	14.26	13.53	13.91
CaO	11.10	10.75	10.70	11.01	10.77
Na_2O	2.36	2.30	2.45	2.42	2.28
K_2O	0.26	0.38	0.35	0.35	0.31
Cl	0.04	0.08	0.05	0.06	0.03
F	0.14	0.23	0.37	0.37	0.05
H_2O	1.99	1.90	1.83	1.83	2.02
F=O	-0.06	-0.10	-0.16	-0.16	-0.02
Cl=O	-0.01	-0.02	-0.01	-0.01	-0.01
Total	100.00	99.73	99.52	99.56	99.92

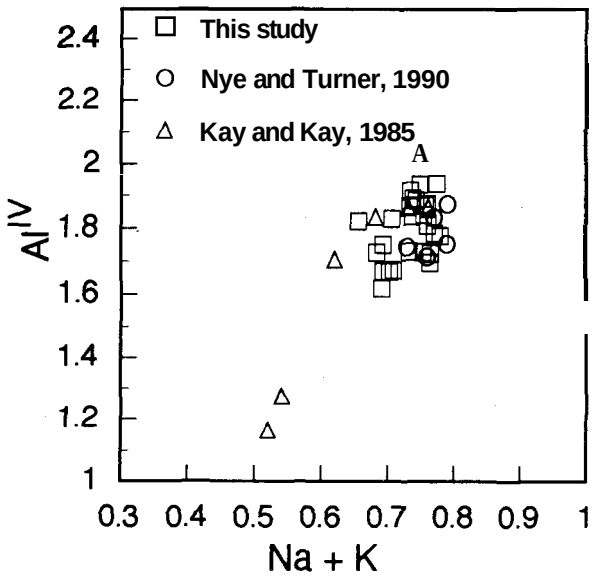

Figure 4. Al(IV) versus Na + K for hornblende of this study and hornblende from Mount Spurr and other Aleutian volcanoes from Nye and Turner (1990) and Kay and Kay (1985).

OPAQUE MINERALS

Opaque minerals are dominantly magnetite, but include a trace amount of pyrrhotite, and they may make up as much as 5 percent of the mode (dense rock). Magnetite occurs as anhedral to subhedral crystals less than 0.2 mm in maximum dimension. Pyrrhotite occurs as anhedral masses as much as 0.5 mm in maximum dimension.

CRYSTAL CLOTS

Small (≤ 2 mm) crystal clots of different minerals are found in all samples (1–2 percent of the mode). The most common clots are (1) plagioclase and magnetite; (2) orthopyroxene and magnetite; (3) plagioclase, orthopyroxene, and magnetite; and (4) poikilitic hornblende and plagioclase. Clinopyroxene is also present in some clots. The pyroxene crystals are subhedral to anhedral, whereas the plagioclase is subhedral to euhedral and typically somewhat sieved.

XENOLITHS

Metamorphic inclusions are present in many samples. The inclusions are of three types: (1) plagioclase and spinel±FeTi oxides, (2) polycrystalline quartz, and (3) plagioclase, quartz, sillimanite, spinel, FeTi oxides, pyrrhotite±biotite±cordierite±corundum. Grains of cordierite are present in some andesites and are probably derived from xenoliths. Nye and Turner (1990) also described plagioclase-spinel clots in Mount Spurr lavas, which they inferred to be altered anorthosite. The ubiquitous nature of spinel in the large metamorphic blocks suggests that they are of metamorphic origin. Xenoliths of older volcanic material are also present in some samples.

DISCUSSION

The brown-black and greenish-gray andesites are petrographically and geochemically similar (Nye and others, this volume); they differ only in their groundmass glass compositions. Groundmass glass compositions in the brown-black andesite from the June and August eruptions are nearly identical. However, in the samples from the September eruption the dominant glass is more silicic and the compositions shift relative to those of samples from the June and August eruptions (fig. 1). This shift in the dominant melt composition from August to September could possibly be the result of progressive crystallization. Presumably this crystallization occurred in the magma body throughout the eruption sequence. Thus, the shift in melt composition suggests the presence of a single magma body undergoing progressive crystallization and tapped for three eruptions. The presence of a single magma body is supported by the geochemistry of the andesite (Nye and others, this volume).

The rhyolitic groundmass glasses from the August and September eruptions also show identical compositional ranges (fig. 1). This observation suggests that the same process generated andesite with rhyolitic groundmass glass in August and September.

Differences in the groundmass glass compositions also result in differences in the range of plagioclase and orthopyroxene compositions. The brown-black andesite with both andesitic and dacitic glasses has plagioclase rim compositions from An_{84} to An_{56}, whereas in the greenish-gray andesite with rhyolitic glass rim compositions are very sodic and extend to An_{22}. The orthopyroxene in samples with andesitic and dacitic glass has rim compositions of En_{61-74} and in the rhyolitic glass samples, En_{49-73}.

There are three possible mechanisms to explain the origin of the various glasses and the resulting sympathetic plagioclase and orthopyroxene compositional differences. These mechanisms are fractional crystallization, assimilation, and magma mixing. Incorporation of more felsic material either through melting of continental crust (assimilation) or magma mixing could cause changes in the melt and crystallizing phases. However, the similarity of andesite geochemistry argues for a closed system (Nye and others, this volume) during the eruption sequence. Therefore, the more

likely explanation is fractional crystallization. Groundmass glass major-element variation diagrams (fig. 5) show predominantly linear trends between the andesitic and rhyolitic glasses, with the exception of Na_2O and MgO. Na_2O vector modeling of plagioclase crystallization indicates it would be possible to drive glass compositions from the dacitic glass to rhyolitic glass through crystallization of plagioclase with compositions of approximately An_{35-45}.

Hornblende phenocrysts, although identical in composition, are stable in the andesitic glasses and to a degree in the dacitic glasses, but they are clearly unstable in the rhyolitic glasses. There are three possible explanations for this: differences in water content of the different glasses (melts); the peraluminous nature of the rhyolitic melts; and reaction kinetics (Rutherford and Hill,1993). It is unclear which of these three mechanisms is the most likely explanation.

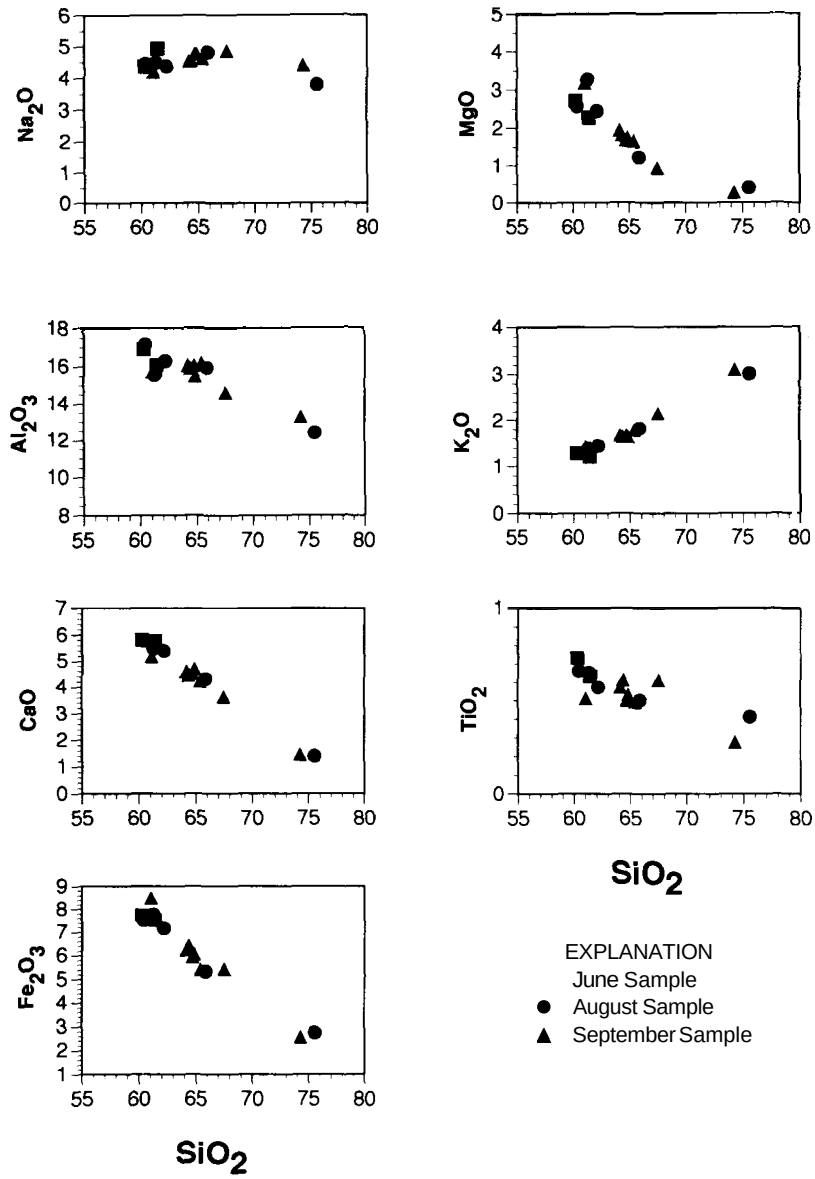

Figure 5. Average groundmass glass compositions (in weight percent) of major oxides plotted against weight percent SiO_2. Glass from andesite samples collected following three eruptions of Mount Spurr, Alaska, in 1992.

SUMMARY

The 1992 eruptions of Mount Spurr provided several types of products for examination, including two types of andesite. Derivation of the greenish-gray andesite with rhyolitic glass appears to have been accomplished through fractional crystallization of brown andesite with andesitic glass. Fractional crystallization is supported by the compositional changes observed in plagioclase and orthopyroxene. Examination of the andesite groundmass glasses suggests that a single magma body undergoing progressive crystallization was present. It seems likely that progressive crystallization took place as microphenocrysts and microlites. Work will be done on groundmass crystallinity to determine any differences.

The role of the metamorphic xenoliths in the Crater Peak magmatic system is not understood. The system was apparently closed during the eruption sequence so any affect on the magma must have occurred prior to the June eruption. Nye and Turner (1990) suggested that crustal sweats have influenced the Mount Spurr magmatic system. The presence of the xenoliths suggests that they are the origin of these crustal sweats. Future work will involve characterizing the xenoliths to determine their role.

REFERENCES CITED

Alaska Volcano Observatory, 1993, Mt. Spurr's 1992 Eruptions: Eos, Transactions of the American Geophysical Union, v. 74, no. 19, May 11,1993, p. 217 and 221–222.

Daley, E.E., 1986, Petrology, geochemistry, and the evolution of magmas from Augustine Volcano, Alaska: M.S. thesis, University of Alaska Fairbanks, p. 106.

Fisher, R.V., and Schmincke, H.-U., 1984, Pyroclastic rocks: New York, Springer-Verlag, p. 472.

Hawthorne, F.C., 1981, Crystal chemistry of the amphiboles, in Veblen, D.R., ed., Amphiboles and other hydrous pyriboles—Mineralogy. Mineralogical Society of America Reviews in Mineralogy, v. 9A, p. 1–102.

Kay, S.M., and Kay, R.W., 1985, Aleutian tholeiitic and calcalkaline magma series I: The mafic phenocrysts: Contributions to Mineralogy and Petrology, v. 90, p. 276–290.

Lindsley, D.H., 1983, Pyroxene thermometry: American Mineralogist, v. 68, p. 477–493.

Nye, C.J., and Turner, D.L., 1990, Petrology, geochemistry, and age of the Spurr volcanic complex, eastern Aleutian arc: Bulletin of Volcanology, v. 52, p. 205–226.

Rutherford, M.J., and Hill, P.M., 1993, Magma ascent rates from amphibole breakdown: An experimental study applied to the 1980–1986 Mount St. Helens eruption: Journal of Geophysical Research, v. 98, p. 19,667–19,685.

Swanson, S.E., Nye, C.J., and Miller, T.P., 1994, Geochemistry of the 1989–1990 eruption of Redoubt Volcano: part II. mineral and glass chemistry, in Miller, T.P., and Chouet, B.A., eds., The 1989–1990 eruptions of Redoubt Volcano, Alaska. Journal of Volcanology and Geothermal Research, v. 62, p. 453–468.